Analysis of Data Harvesting by Unmanned Aerial Vehicles

Chang-sik Choi
Department of ECE
UT Austin
2501 Speedway, Austin, TX 78712
Email: chang-sik.choi@utexas.edu

François Baccelli
Department of ECE and Math
UT Austin
2501 Speedway, Austin, TX 78712
Email: baccelli@math.utexas.edu

Gustavo de Veciana
Department of ECE
UT Austin
2501 Speedway, Austin, TX 78712
Email: gustavo@ece.utexas.edu

***Abstract*—This paper explores an emerging wireless architecture based on unmanned aerial vehicles (UAVs), i.e., drones. We consider a network where UAVs at fixed altitude harvest data from Internet-of-Things (IoT) devices on the ground. Each UAV serves IoT devices within its coverage area. In such a system, the UAVs' motion activates IoT uplink transmissions and so the motion triggers the interference field and determines the network performance. To analyze the performance, we propose a stochastic geometry model. The coverage area of each UAV, referred to as the activation window, is modeled for simplicity as a rectangle where at most one IoT device is scheduled to transmit at any given time. In this setting, we analyze the signal-to-interference and data rate from two typical perspectives, namely from a typical UAV's and from a typical IoT device's points of view.**

I. Introduction

This paper focuses on an aerial-based network enabling the connectivity to ground-based Internet-of-Things devices (IoT) [1]. When IoT devices have a limited transmission range, the data from IoT devices could be collected with the help of technologies such as narrowband-IoT [2] and low-power-wide-area [3]. Yet, these approaches are based on a fixed infrastructure and, as pointed out in several papers including [4], the network capacity may be limited as the density of IoT devices increases.

In the context of network densification, a possible approach is to leverage mobile elements such as vehicles. Underlying such a network architecture is the delay tolerant concept [5]–[7], where the network capacity or coverage are improved by possibly tolerating additional delays. As discussed in the literature [8], a number of IoT applications are delay tolerant and therefore rely on vehicles would be a conceivable mean to harvest information from IoT devices. To that end, technologies that utilize mobile harvesters or data mules have been studied in [9]–[12].

Nevertheless, IoT data harvesting via vehicles undergoes a few practical limitations. First, vehicles travel only on roads and thus vehicles may fail to provide sufficient coverage if IoT devices are far from the roads. Second, the quality of communication diminishes as the distance from vehicles to IoT devices grows, especially for static IoT devices [13]. An emerging technology which overcomes these challenges is that based on Unmanned Aircraft Vehicles (UAVs), e.g., drones; Indeed, motion is no longer limited to the road network. Furthermore, UAVs' trajectories can be orchestrated to enhance network performance. Given this advantage over vehicles, they have drawn attention from various industry players. Amazon Prime Air [14] and Google Wing [15] are two such examples. UAVs have been studied by academia and industry as a key network enabler [16], [17]. The aim of the paper is to explore the emerging wireless architecture where UAVs harvest IoT data from ground IoT devices.

It is challenging to analyze the performance of such networks because the links are established between *fixed* IoT devices and *flying* UAVs, instead of between fixed IoT devices and fixed base stations, for example. Consequently, the analysis of the network performance should be based on a system model that captures the relative motion of the UAVs and IoT devices. In such a network, the motion of UAVs drives the activation of the uplink transmission/interference and thus the network performance.

The contributions of this paper are as follows:

An analytical framework for Data Harvesting based on UAV network: This paper proposes a new architecture where constantly moving UAVs collect IoT data from surface-level devices. We use two stationary point processes to model the locations of IoT devices and UAVs, respectively. We initially study a linear UAV network. The locations of UAVs are modeled as a randomly shifted periodic point process. UAVs move at speed v to the positive x-direction. Surface IoT devices are assumed to be distributed according to a homogeneous Poisson point process with intensity λ in a strip of size l centered on the x-axis. Each UAV activates IoT devices in its coverage area homogeneously and at most one device from each coverage area is allowed to transmit at a time. The motion of UAVs steers the coverage areas on the ground. Consequently, the data transmissions, interference, and network performance are driven by the mobility and geometry of the network model.

Performance analysis of the coverage probability, data rate, and amount of transmitted data: We begin by showing that the shot-noise process (and the interference power) at a typical UAV is translation- and time-invariant. Then, under the Palm distribution of the UAV point process, we obtain the SIR distribution of the typical UAV as well as its data

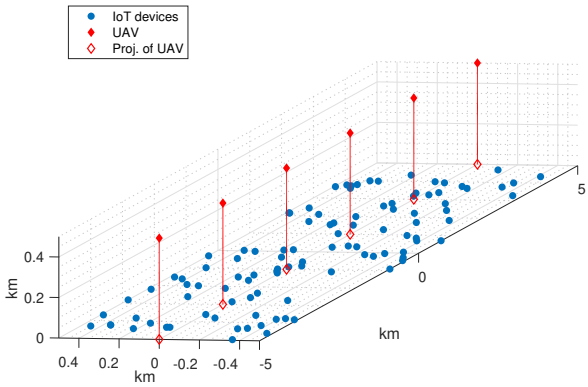

Fig. 1. Illustration of the proposed model where the UAVs are at the height $z = 0.5$ km and the distance between UAVs is 2km.

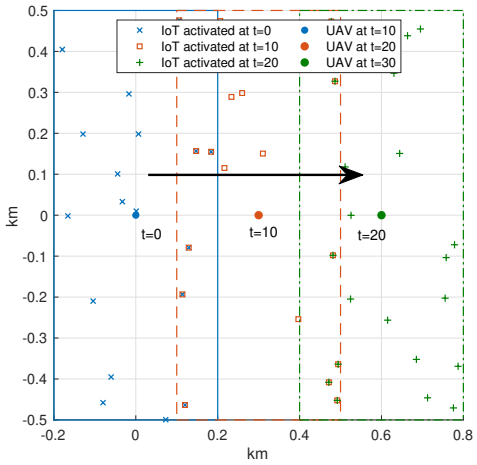

Fig. 2. Illustration of the proposed network with a UAV located at $(0, 0, h)$ at time zero. The black arrow indicate the moving direction. It moves at 108 km/h and the density of IoTs is 100km^2. The activation windows at time $t = 0, 10, 20$ are described by solid blue, dashed red, dotted green rectangles, respectively.

rate. Similarly, under the Palm distribution of the IoT point process, we characterize the amount of data transmitted from the typical IoT device to its serving UAV. By comparing the network performance from two points of view, we formulate a general relationship that the data rate of the typical UAV and the amount of data transmitted from the typical IoT device is linearly related. The formula follows from the mass transport principle, which implies that it holds for any spatial model having joint stationary structure.

II. System Model

We begin by introducing our spatial model for the proposed UAV network. Then, we discuss access control, propagation model, and network performance metrics.

A. UAVs and IoT Devices

IoT devices on the ground are distributed according to a planar Poisson point process of intensity λ on a bi-infinite strip of width l on the x, y plane. The finite width strip allows us to focus our analysis on the relative motion of UAVs and IoT devices and then on uplink communications from IoT devices to UAVs. The IoT devices are assumed to be static and to always have data to transmit.

To model the locations of UAVs, we use a randomly-shifted periodic point process on a line; UAVs are separated by distance μ. The locations of UAVs at time t are given by

$$\Psi(t) = \sum_{k\in\mathbb{Z}} \delta_{(k\mu,0,h)+(U,0,0)+(vt,0,0)}, \tag{1}$$

where $U \sim \text{Uniform}\left[-\frac{\mu}{2}, \frac{\mu}{2}\right]$ is a random uniform shift, μ is the distance between UAVs, δ_x denotes the Dirac measure indicating a point mass at location x, $\mathbb{Z}$ denotes the set of all integers, and h is the UAVs' altitude. UAVs move with speed of v. Fig. 1 illustrates the UAVs, their projections, and the IoT devices. Due to the shift U, the proposed UAV point process is stationary. [18].

B. Multiple Access

In the network based on UAV harvesters, the uplink transmissions from IoT devices are driven by the motion of UAVs. To begin with, an IoT device is marked as active if and only if it is located inside the coverage area of UAV—referred to as the activation window. It is given by the set $[-\frac{w}{2}, \frac{w}{2}]\times[-\frac{l}{2}, \frac{l}{2}]$ centered at every projection of UAV onto the ground.

We assume that time is slotted. From each activation window, out of its all active IoT devices, a single IoT device is randomly chosen for data transmission. In other words, at each time, IoT devices insides the windows are activated as possible candidates for data transmission, yet at most one IoT device per window transmits at a time. Such an access control model can be interpreted as time division multiple access (TDMA) scheduling by the UAV, which will later be approximated by a processor sharing scheme; we will refer to it simply as TDMA. Fig. 2 illustrates the locations of IoT devices, activation windows at time $0, 10,$ and $20,$, and corresponding active IoT devices, respectively.

C. Propagation Model

Time is slotted and we assume that each time slot has a duration T_s. Each time slot is assumed to be equal to the coherence time T_c of the wireless channel. Consequently, each time slot experiences a different realization of a Rayleigh fading.

The received signal power is modeled by a distance-based power law path loss model with Rayleigh fading. Specifically, the received signal power over distance d is equal to $pGd^{-\alpha}$ where p is the transmit power, G is an exponential random variable with mean one, and α is the path loss exponent greater than one [19].

D. Performance Metrics

For the proposed UAV network, we evaluate the performance from two typical perspectives: UAV's perspective and IoT device's perspectives. For each perspective, we use different Palm distributions and then analyze the coverage probability and instantaneous data rate.

III. Performance from UAVs

A. Shot-noise process seen by the typical UAV

To quantify the shot-noise process seen by the typical UAV, we consider the Palm distribution of the UAV point process. Under this Palm distribution, a typical UAV is located at $(0, 0, h)$ at any given slot [20]. Consequently, corresponding activation windows for all UAVs are given by

$$\mathcal{W} = \bigcup_{i\in\mathbb{Z}} \mathcal{W}_i = \bigcup_{i\in\mathbb{Z}} \left[\mu i - \frac{w}{2}, \mu i + \frac{w}{2}\right] \times \left[-\frac{l}{2}, \frac{l}{2}\right].$$

Under the TDMA, the shot-noise process—associated with the uplink transmissions from IoT devices—seen at the typical UAV is given by

$$N = \sum_{i\in\mathbb{Z}} pG_i \|(X_i, Y_i, 0) - (0, 0, h)\|^{-\alpha} \mathbb{1}_{\{\Phi(\mathcal{W}_i)\neq\emptyset\}},$$

where (X_i, Y_i) are the x and y coordinates of the transmitting IoT device, if any, in window $\mathcal{W}_i$. Let $\hat{\Phi}$ denote the active IoT point process. Let $\mathbb{1}_{\{A\}}$ denote the indicator function that takes value one only if A is true, or zero otherwise.

Theorem 1. *The Laplace transform of the uplink shot-noise process at the typical UAV is given by Eq.* (2)*.*

Proof: See [21] for the proof. ∎

Remark 1. *The shot-noise process of the typical UAV is time-invariant. This indicates that the distribution of the shot-noise process seen by the typical UAV characterizes that of shot-noise process seen by* any UAV *at* any given time slot*. The shot-noise process directly leads to the interference of the network, and therefore it eventually determines the network performance. Notice that the typical analysis is made possible because of the joint stationarity of the proposed geometry model and the linear motion of UAVs.*

B. Coverage Probability

We assume that each UAV decodes the received signal transmitted from its own window, by treating interference from other windows as noise. The coverage probability is defined as a function of τ: $\mathbf{P}^0_\Psi(\text{SIR} \geq \tau)$ under the Palm distribution of Ψ, where $\text{SIR} = S/I$ and the random variables S and I denote the received signal power, and the interference power, respectively.

Theorem 2. *The coverage probability of the typical UAV is given by Eq.* (3)*.*

Proof: See [21] for the proof. ∎

Fig. 3 illustrates the coverage probability of the typical UAV obtained by analytical formula Eq. (3) and by simulations, respectively. Simulation results confirm the accuracy of the derived formula. The increase of altitude of UAVs decreases the coverage probability of the typical UAV. The coverage probability at arbitrary small τ is equal to $1 - e^{-\lambda w l}$.

Remark 2. *Since the UAV and IoT point processes are joint stationary and the IoT point process is mixing, the above coverage expression can be interpreted in an ergodic sense [20]. The coverage probability accounts for the proportion of time that the UAV correctly decode messages.*

C. Data Rate

This section analyzes the data rate and the spectral efficiency. Let us consider a fixed M-ary modulation with minimum SIR threshold τ. The data rate of the typical UAV is defined by $\log_2(M)\,\mathbf{P}^0_\Psi(\text{SIR} \geq \tau)$.

Theorem 3. *The data rate seen by the typical UAV, $\mathcal{R}$, is given by Eq.* (4)*.*

Proof: The proof follows from Theorem 2. ∎

Figs. 4 and 5 show the typical data rate seen from the typical UAV. The curve on Fig. 4 is not smooth since the modulation is given by $M = 2^{\lfloor \log_2(1+\tau) \rfloor}$ based on the SIR threshold τ. Fig. 5 describes the data rate of the typical UAV with respect to (w.r.t.) various SIR thresholds τ. The data rate is given by $\log_2(1+\tau)\,\mathbf{P}(\text{SIR} > \tau)$ which is the product of increasing and decreasing functions w.r.t. τ, respectively. Based on the network geometry, the best τ can be found by exploiting the trade-off. As in Fig. 5, for τ less than 10 dB, increasing the threshold τ increases the data rate. On contrary, for τ greater than 10 dB, increasing τ decreases the data rate. For the activation window of $w = 0.5$, the optimum threshold is around 20 dB. The SIR threshold τ may be provided as a fixed system parameter in practice, based on the requirement of IoT application.

IV. Performance from IoT Devices

This section focuses on the network performance seen from a typical IoT. Specifically, under the Palm distribution of the IoT point process, we derive the total amount of data transmitted, i.e., harvested from the typical IoT device to a UAV, while the typical IoT device is inside the activation window of the UAV.

A. Transmitted Data from the Typical IoT

The coverage and rate analysis of the previous section captures the instantaneous network performance. Nevertheless, in each activation window, a Poisson number of IoT devices are present for each time slot and the processing of UAV is shared by these IoT devices, based on TDMA. Consequently, in order to compute the total amount of data transmitted from a typical IoT device to a UAV while the IoT device is located inside the activation window of the UAV, i.e., while it is served by this UAV, one should consider the evolution of the network geometry w.r.t. time.

We consider a typical IoT device that is randomly located on the y-axis using the Palm distribution of the IoT point process.

$$\mathcal{L}_N(s) = \prod_{k\in\mathbb{Z}} \left(e^{-\lambda w l} + \frac{1-e^{-\lambda w l}}{wl} \int_{k\mu-\frac{w}{2}}^{k\mu+\frac{w}{2}} \int_{-\frac{l}{2}}^{\frac{l}{2}} \frac{1}{1+\frac{sp}{(x^2+y^2+h^2)^{\alpha/2}}} \,\mathrm{d}y\,\mathrm{d}x \right). \tag{2}$$

$$\mathbf{P}(\mathrm{SIR} > \tau) = \frac{1-e^{-\lambda w l}}{wl} \int_{-\frac{w}{2}}^{\frac{w}{2}} \int_{-\frac{l}{2}}^{\frac{l}{2}} \prod_{k\in\mathbb{Z}\setminus 0} \left(e^{-\lambda w l} + \frac{1-e^{-\lambda w l}}{wl} \int_{k\mu-\frac{w}{2}}^{k\mu+\frac{w}{2}} \int_{-\frac{l}{2}}^{\frac{l}{2}} \frac{\mathrm{d}u\,\mathrm{d}v}{1+\frac{\tau(x^2+y^2+h^2)^{\frac{\alpha}{2}}}{(u^2+v^2+h^2)^{\frac{\alpha}{2}}}} \right) \mathrm{d}y\,\mathrm{d}x. \tag{3}$$

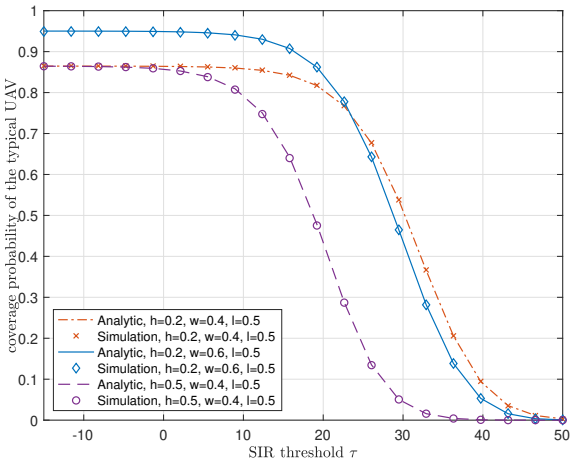

Fig. 3. Coverage probability of the typical UAV. We consider $\alpha = 4$.

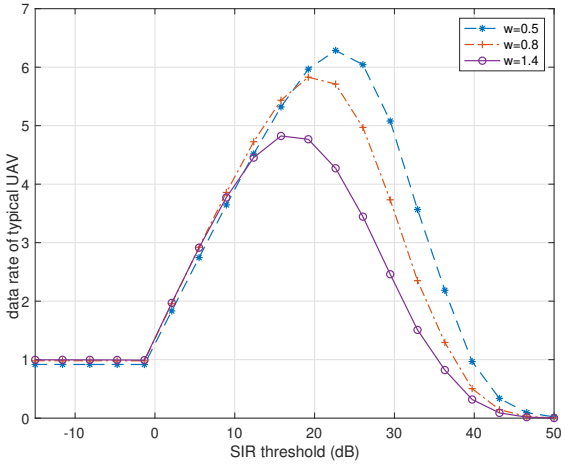

Fig. 5. The data rate seen from the typical UAV. We assume that $\alpha = 4$ and $M = 2^{\lfloor \log_2(1+\tau) \rfloor}$.

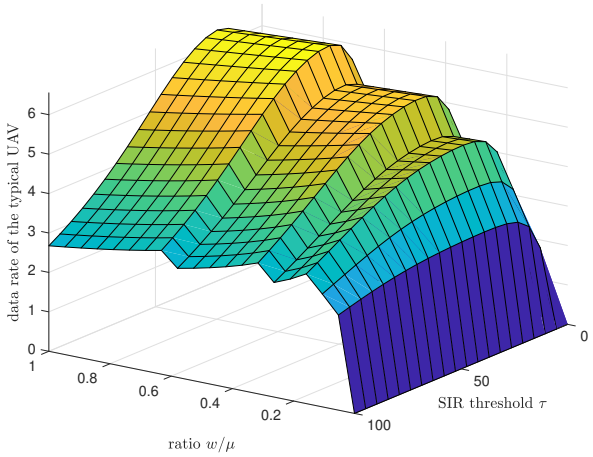

Fig. 4. The data rate at the typical UAV where a typical M-ary modulation is assumed: $M = 2^{\lfloor \log_2(1+\tau) \rfloor}$ with threshold τ.

We then derive the formula for the amount of data transmitted from the typical IoT device to its serving UAV, namely the amount of data transmitted from the typical IoT device per UAV passage.

Theorem 4. *The amount of data $\mathcal{D}$ transmitted from the typical IoT device per UAV passage is given by Eq.* (5).

Proof: See [21] for the proof. ∎

Here are few observations on Theorem 4. (1) $\mathcal{D}$ is inversely linear with the speed of UAVs v. If the typical UAV moves faster, it provides a shorter duration of active time for the typical IoT device, and consequently, the total amount of data transmitted would decrease. (2) $\mathcal{D}$ is monotonically increasing with the distance between UAVs, μ. As the distance between UAVs increases, the interference power decreases, and thus the coverage and rate increase. (3) $\mathcal{D}$ is decreasing with the density of IoTs λ. As the density increases, the number of active IoT devices per window increases, and therefore $\mathcal{D}$ diminishes due to the TDMA between the more numerous IoT devices.

V. UAV Network Optimizaiton

The activation windows are modeled as a collection of rectangles on the plane. The width l of rectangles is derived from the deployment of IoT devices and thus corresponds to the area of interest. The length of each window w, on the other hand, is a parameter that may be optimized to achieve the best overall network performance.

Various performance metrics behave in different ways when varying w. We focus on $\mathcal{R}$. For instance, if w is too big, IoT devices far from UAVs would be activated and therefore the received signal power of the signal component would decrease. On the other hand, if the window w is too small, the chance of activation window to be empty of IoT devices would increase and therefore the data rate would diminish. Consequently, there exists an optimum window size w that

$$\mathcal{R} = \frac{(1-e^{-\lambda w l})\log_2(M)}{wl} \int_{-\frac{w}{2}}^{\frac{w}{2}} \int_{-\frac{l}{2}}^{\frac{l}{2}} \prod_{k\in\mathbb{Z}\setminus 0} \left(e^{-\lambda w l} + \frac{1-e^{-\lambda w l}}{wl} \int_{k\mu-\frac{w}{2}}^{k\mu+\frac{w}{2}} \int_{-\frac{l}{2}}^{\frac{l}{2}} \frac{\mathrm{d}u\,\mathrm{d}v}{1+\frac{\tau(x^2+y^2+h^2)^{\frac{\alpha}{2}}}{(u^2+v^2+h^2)^{\frac{\alpha}{2}}}} \right) \mathrm{d}y\,\mathrm{d}x. \tag{4}$$

$$\mathcal{D} = \frac{(1-e^{-\lambda w l})\log_2(M)}{v\lambda w l^2} \int_{-\frac{w}{2}}^{\frac{w}{2}} \int_{-\frac{l}{2}}^{\frac{l}{2}} \prod_{k\in\mathbb{Z}\setminus 0} \left(e^{-\lambda w l} + \frac{1-e^{-\lambda w l}}{wl} \int_{k\mu-\frac{w}{2}}^{k\mu+\frac{w}{2}} \int_{-\frac{l}{2}}^{\frac{l}{2}} \frac{\mathrm{d}u\,\mathrm{d}v}{1+\frac{\tau(x^2+y^2+h^2)^{\frac{\alpha}{2}}}{(u^2+v^2+h^2)^{\frac{\alpha}{2}}}} \right) \mathrm{d}y\,\mathrm{d}x. \tag{5}$$

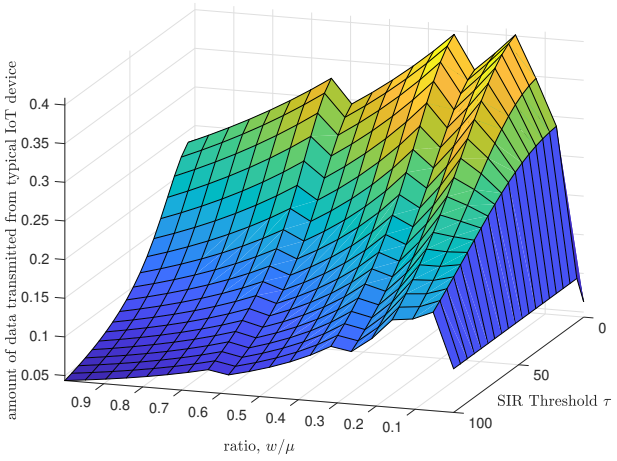

Fig. 6. Amount of data transmitted from the typical IoT device to the typical UAV. We consider $\alpha = 2.5, h = 0.2$ km, $\mu = 2$ km, $l = 0.5$ km, $v = 72$ km/h, and $\lambda = 1000/\text{km}^2$.

maximizes $\mathcal{R}$. For a given SIR threshold τ, the optimization problem is formulated as

$$\arg\max_{0<w<\mu} \mathcal{R},$$

and the optimization is discussed in [21].

VI. Conclusion

This paper provides a framework to analyze the performance of data harvesting from IoT devices on the building tops or ground to a network of UAVs. Using stochastic geometry, we propose a spatial model to describe the locations and movement of IoT devices and UAVs. The coverage probability of the typical UAV and its data rate are derived. Then, we compute the amount of data transmitted from the typical IoT device.

References

[1] J. Gubbi, R. Buyya, S. Marusic, and M. Palaniswami, "Internet of things (IoT): A vision, architectural elements, and future directions," *Future generation computer systems*, vol. 29, no. 7, pp. 1645–1660, July 2013.

[2] Y. . E. Wang, X. Lin, A. Adhikary, A. Grovlen, Y. Sui, Y. Blankenship, J. Bergman, and H. S. Razaghi, "A primer on 3GPP narrowband internet of things," *IEEE Commun. Mag.*, vol. 55, no. 3, pp. 117–123, March 2017.

[3] R. S. Sinha, Y. Wei, and S.-H. Hwang, "A survey on LPWA technology: LoRa and NB-IoT," *Ict Express*, vol. 3, no. 1, pp. 14–21, Mar. 2017.

[4] A. Zemlianov and G. de Veciana, "Capacity of ad hoc wireless networks with infrastructure support," *IEEE J. Sel. Areas Commun.*, vol. 23, no. 3, pp. 657–667, Mar. 2005.

[5] M. Grossglauser and D. N. Tse, "Mobility increases the capacity of ad hoc wireless networks," *IEEE/ACM Trans. Netw.*, vol. 10, no. 4, pp. 477–486, Aug. 2002.

[6] K. Fall and S. Farrell, "DTN: an architectural retrospective," *IEEE J. Sel. Areas Commun.*, vol. 26, no. 5, pp. 828–836, June 2008.

[7] A. Abdrabou and W. Zhuang, "Probabilistic delay control and road side unit placement for vehicular ad hoc networks with disrupted connectivity," *IEEE J. Sel. Areas Commun.*, vol. 29, no. 1, pp. 129–139, Jan. 2011.

[8] P. R. Pereira, A. Casaca, J. J. Rodrigues, V. N. Soares, J. Triay, and C. Cervello-Pastor, "From delay-tolerant networks to vehicular delay-tolerant networks," *IEEE Commun. Surv&Tuts*, vol. 14, no. 4, pp. 1166–1182, Fourth 2012.

[9] E. W. Saad, J. L. Vian, M. A. Vavrina, J. A. Nisbett, and D. C. Wunsch, "Vehicle base station," Dec 2014, U.S. Patent no. 8,899,903.

[10] M. Talluri, K. Agarwal, R. K. Mishra, and S. Garg, "Enhanced mobile base station," Mar 2018, U.S. Patent no. 9,913,095.

[11] C. Choi, F. Baccelli, and G. de Veciana, "Densification leveraging mobility: An IoT architecture based on mesh networking and vehicles," in *Proc. ACM MobiHoc*, 2018, pp. 71–80.

[12] C. Choi and F. Baccelli, "Modeling and optimization of direct communications from IoT devices to vehicles," in *Proc. IEEE Globecom Workshops*, Dec. 2018, pp. 1–7.

[13] ——, "Poisson cox point processes for vehicular networks," *IEEE Trans. Veh. Technol.*, vol. 67, no. 10, pp. 10 160–10 165, Oct 2018.

[14] Amazon, "Amazon Prime air," 2016, https://www.amazon.com, visited 2018-09-26.

[15] Google, "Google project wing," 2016, https://x.company/projects/wing/, visited 2018-09-26.

[16] X. Lin, V. Yajnanarayana, S. D. Muruganathan, S. Gao, H. Asplund, H.-L. Maattanen, M. Bergstrom, S. Euler, and Y.-P. E. Wang, "The sky is not the limit: LTE for unmanned aerial vehicles," *IEEE Commun. Mag.*, vol. 56, no. 4, pp. 204–210, 2018.

[17] S. D. Muruganathan, X. Lin, H.-L. Maattanen, Z. Zou, W. A. Hapsari, and S. Yasukawa, "An overview of 3GPP release-15 study on enhanced LTE support for connected drones," *arXiv preprint arXiv:1805.00826*, 2018.

[18] F. Baccelli, B. Błaszczyszyn *et al.*, "Stochastic geometry and wireless networks: Volume I theory," *Foundations and Trends® in Networking*, vol. 3, no. 3–4, pp. 249–449, 2010.

[19] F. Baccelli and A. Biswas, "On scaling limits of power law shot-noise fields," *Stochastic Models*, vol. 31, no. 2, pp. 187–207, 2015. [Online]. Available: https://doi.org/10.1080/15326349.2014.990980

[20] F. Baccelli and P. Brémaud, *Elements of queueing theory: Palm Martingale calculus and stochastic recurrences*. Springer Science & Business Media, 2013, vol. 26.

[21] C. Choi, F. Baccelli, and G. de Veciana, "Analysis of unmanned aerial vehicle networks for data harvesting." [Online]. Available: https://www.dropbox.com/s/jtrwy38svgxv3i6/MCN_drone_v7.pdf?dl=0